Comparable Analysis on Frequency Selective Surface (FSS) Structures using Finite FDTD in FORTRAN and CST

H. Nornikman[1], N. C. Pee[2], B. H. Ahmad[1], S. N. Salleh[1], M. Z. A. Abd Aziz[1]
[1]*Center for Telecommunication Research and Innovation (CeTRI), Faculty of Electronics and Computer Engineering (FKEKK), Universiti Teknikal Malaysia Melaka (UTeM), Durian Tunggal, Melaka, Malaysia*
[2]*Faculty of Information and Communication Technology (FTMK), Universiti Teknikal Malaysia Melaka (UTeM), Durian Tunggal, Melaka, Malaysia*
nornikman@utem.edu.my

***Abstract*—In this work, two dissimilar forms of frequency selective surface (FSS) shaped are consider designing in Computer Simulation Technology (CST) and FORTRAN simulator. Square loop FSS is the first design and followed by the cross dipole FSS. The works start using Genetic Algorithm (GA) as the optimization tool to generate bits of the chromosome in designing the shape of energy-saving glass (ESG). Then, another way is using the Finite Difference Time Domain (FDTD) was working as a design the complicated shape in pixelized shape based on the unit cell thought. For the result, it can compare on several performance parameters. Firstly, in CST, the results of S21 shown - 43.2 dB as resonant frequency is at 12.8 GHz. For FORTRAN simulator, it shows the performance of - 68.1 dB at 12.8 GHz of resonant frequency.**

***Index Terms*— frequency selective surface; Genetic Algorithm; energy-saving glass; Finite Difference Time Domain; Computer Simulation Technology**

I. Introduction

Malaysia is a tropical land with a hot and wet climate all time laterally, with norm 34^0 C of temperature. Energy-saving glass (ESG) functioning in blocking of infrared and ultraviolet light radiation. It capability had been shown in the insertion of transparent metallic oxide coat on one side of the glass on the building [1-2]. This ESG had a capability to control the temperature level indoor and effect of reducing energy used. Low-emissivity (low-E) coating is the other name of metallic oxide coating had functioning to lessen the amount of ultraviolet and infrared ignitor that can pass over glass without conceding the volume of the transmitted observable light source.

Besides that, this ESG are stated as green technology. Subsequently, it evades needless warmth from incoming a building over summer and protective the heat during winter [3]. In addition, even though ESG is normally exploited in the state with four-time of year, such as the European continent, it is also appropriate for universal countries, including near equator line states like Malaysia [4]. By the way, this ESG had been disadvantages to eliminating the many useful microwave and radio frequency (RF) signals. But, for some reason, this signal attenuation can effect to avoid some unwanted signal.

Back to the previous work, the ESG had been designed in such over the world. Habib in his work had been done the investigation of a band-pass FSS for double glazed soft-coated energy-saving glass that achieved - 20 dB performance in the range between 0.1 GHz and 2.3 GHz [5]. On the other hand, Ma introduced a tri-bandpass frequency selective surface (FSS) of ESG in the range of 0.833 GHz – 0.1009 GHz, 1.842 GHz – 2.200 GHz and 3.420 GHz – 4.300 GHz with performance higher than – 3 dB [6]. Sohail successfully designs a dual layer energy saving glass for RF communication in the range between 0.5 GHz to 2 GHz [7]. Last example, Ragulis introduced a wideband ESG with a thin conductive film that operates for microwave frequencies from 1 to 20 GHz [8].

Another two examples are focus in Malaysia. For the first case, Lim had been investigating on the one side of the glass that coated of the tin oxide (SnO_2) for thermal insulation purpose. This work is operating in between 0.8 GHz and 2.2 GHz [9].

Mohamad had been researching on the energy performance in a Green Energy Office (GEO) building in Putrajaya, Malaysia. This building had been built to as a decision of Malaysian government under Ministry of Energy, Green Technology and Water in 2004 by Low Energy Office (LEO) building law [10].

Frequency selective surface (FSS) is a radio frequency (RF) filter with a dielectric substrate that containing of an array of periodic metallic patches. Inductive FSS or capacitive FSS basically had the ability to pass or block the waves of convinced frequencies in free space. The FSS structure had been used in many applications such as a part of antenna design, metamaterial microwave absorber, and others RF application that using in electromagnetic interference, terahertz application, and radar cross-section.

The length of the element of this FSS structure is a various of half of the resonant wavelength ($\lambda g/2$) [11]. Due to the relative frequency selective surface feature, which is narrowband and periodic in 2D, FSS is joint to be used in a wide variety of equipment or purpose, such as the realization of a reflector antenna, arbitrary design, and cross radomes [12]. Table 1 demonstrates the several designed of regular covering glasses shapes ESG. These characters contain dipole antenna, cross dipole, double square dipole, and many other shapes. The glass and the metallic oxide coating is differentiating by the red and yellow color, respectively.

Normal shape FSS coverings layers have been presented as the explanation to overwhelm the loss of the signal of RF with ESG structure. On the other hand, the normal shape is signified whilst all the edges of the shapes have the equal length and angle standards that must be same for all the angles. The modern procedures and investigator approximately the numerous designs of normal form, which includes dipole, double rectangular loop, and different shapes, have exact to growth the transmission sign (S_{21}) of convenient sign and on the similar time, to lessen signal attenuation.

Aside from that, previous work by another designer mostly converted the design of normal shape into an alternative shape that makes use of the simple regular form which will acquire the high-quality transmission signal (S_{21}). From the preceding work by other researchers, there are many of fundamental shaped stated, such as regular shapes are cross dipole [13-15], Jerusalem [16-18], and double square loop [19-20]. As a sample, a double rectangular loop shape, that's designed inside the rectangular loop form, is an addition to the second layer for another square loop where each shape is nonetheless a regular form.

Table 1. regular ESG with glass and metallic oxide coating

Researcher, year	Design shape	Remarks
(Kiani, 2008) [21]	Square dipole shape 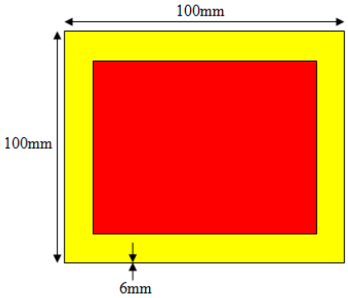	Using CST simulator
(Esselle, 2011) [22]	Double square dipole shape 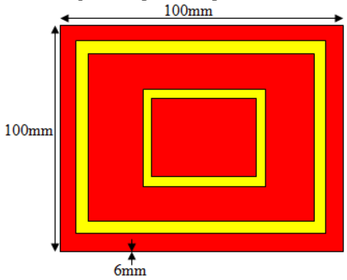	Blend between two regular square shapes
(Olsson, 2011) [23]	Cross dipole shape 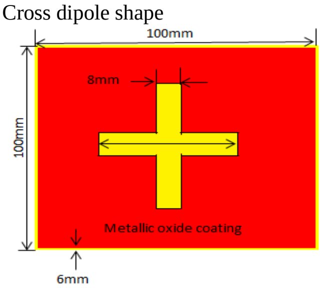	Cross dipole is a mixture between square and rectangular shapes

The example form that was considered to improve the transmission signal of ESG have been the cross-dipole form, that's indeed a normal shape by way of Kiani [21] in 2008. Cross dipole aperture became designed for the coated side for periodic unit mobile. This aperture became indifferent out from the lined to reduce the lessening of useful RF/microwave signal to skip thru the ESG for the complete band from 500 MHz to 6 GHz. The advance growth of this transmission coefficient of ESG at 1.3 GHz, 2.45 GHz, and 5 GHz were - 9 dB, - 5.25 dB, and - 4 dB, respectively.

Within the different works, in 2011, Ranga and Esselle [22] were studies on the rectangular shape that combined with added square form in a single layout. It shows that the double square loop shape is convenient with the microwave signal and it changed into executed from 500 MHz to six GHz for GSM software, which turned into altered from 900 MHz to 1800 MHz and a wireless local area network (WLAN) utility for 2.45 GHz and 5.25 GHz.

Olsson [23] in 2008 had been investigating the square loop at four different frequencies at 0.9 GHz, 1.8 GHz, 2.45 GHz and 5.25 GHz, focusing on the frequency range for ESG applications. This transmission was for vertical (TE) polarization from 0° to 60° angles of incidence.

Azemi [24] had been introduced the 3D FSS with array ring unit element with the cylinder shape that operates in the band stop region range from 2.56 GHz to 2.67 GHz. Sharma in 2017 presented his work on the small Ku band F-shaped patch antenna that using the FSS structure that applies between 12.0 GHz and 18.0 GHz [25].

Bodur [26] design a 12×12 reflectarray antenna that using double layer FSS with a resonant frequency range between 2.0 GHz and 12.0 GHz. This structure effect to a decrease of radar cross section (RCS) compares with a reflect array antenna without FSS. The alternative works at the FSS are stated by Lee [27]. His study focusses on the effect of the square loop FSS structure as a filter to attenuate other than WLAN (2.4 GHz) signal.

The prevailing tools, along with the Computer Simulation Technology (CST) Microwave Studio simulator has restriction in its feature, in time of fixing attenuation (mesh cell ability within the software program) since complex form could be difficult to form which create the designing method tough where the complicated form involves small pixels, and it's complex to design and enhance each single pixel.

Therefore, this studies design two distinctive varieties of frequency selective surface of rectangular loop FSS and go dipole FSS. Distinctive tool was applied to design a complex form by means of the use of Genetic algorithm (GA) as the optimization device to generate bits of chromosome in designing the shape of ESG, whilst the Finite-difference Time-domain (FDTD) was hired as a technique of numerical set of rules modeling to design the complex shape in pixelized form primarily based on the cellular unit concept.

II. Algorithm Method

This segment stated on the substances and the approaches that had been applying in this study. It portrays the method applied to broaden the simulator tool for designing the FSS form structure until simulation of the shape primarily based on the approach defined within the preceding segment. This procedure clarifies how the simulator tool produced the FSS layout by making use of the aggregate among both strategies; which have been Finite difference Time-domain (FDTD) as the numerical modeling technique and Genetic algorithm (GA) as the optimization tool to be able to suggest the random (complex) FSS design form of ESG. FDTD has a capability to solve the various electromagnetic wave calculation in the time domain.

Zhang [28] in his paper done the investigation on the periodic structure using this two-different method of split-field FDTD and Spectral FDTD. Chen [29] in his paper apply the alternating-direction-implicit finite FDTD technique for tunable graphene-based FSS in terahertz frequency range. On the other hand, Shunxi [30] had been evaluating the periodic structures by oblique incident electromagnetic wave using this FDTD technique. His design is applying for a double-layered dielectric plate at millimeter wavelengths.

The key program ESGCPML in evolving the tool starts with module Preprocess where the subroutine *FetchNumberFileTherefore*, work to design the structure in 3D without generating the ESG structure, by reading file "*InputTXT\PremierFichier.txt*". The ESG structure without the item, as depicted in Figure 1.

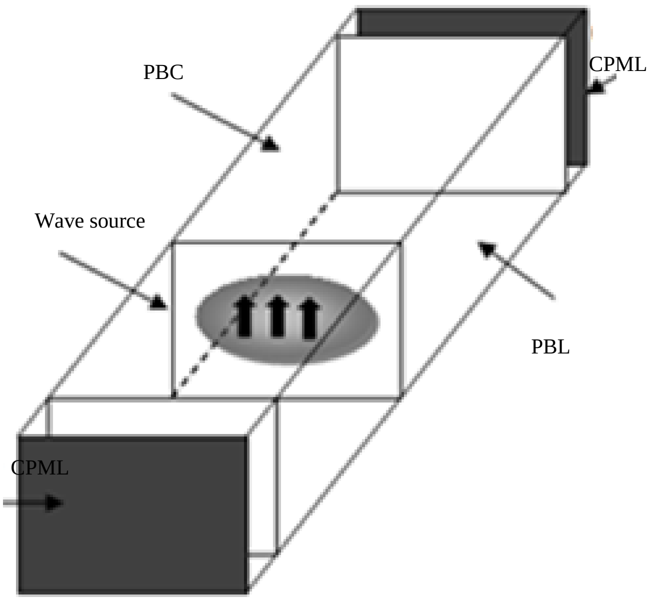

Figure 1. Modelling structure without ESG item inside the structure

The approach concerned the system of 3-d FDTD for a unit cell with ESG, which protected the idea of FDTD and Maxwell's equation that confined Faraday's regulation and Ampere's law in growing three-D FDTD systems of unit cellular.

The calculation of FDTD replicated the discretization of the magnetic and electric field of battle in Maxwell's scalar par for both spatial and time domains. This FDTD allowable the boundary condition on the outer margin of the domain to simulate its extension phone to infinity and to block the mirror image of the outgoing wave to avoid the presence of those affected by reflected waves of the modelled bodily structure.

The components of FDTD imitated the discretization of magnetic and electric powered fields in Maxwell's scalar equations for both spatial and time domain names. They permitted the boundary situation at the outer perimeter of the area to pretend its extension to infinity and to dam the mirrored image of the outgoing wave to keep away from the presence of these stricken by pondered waves of the modelled structures.

Equation (1) to Equation (6) exposed on the FDTD equation for Electrical Field in x,y,z-axis and FDTD equation for Magnetic Field in x,y,z-axis.

FDTD equation for Electric Field in x-axis:

$$
\begin{aligned}
E_x^{n+1}(i,j,k) = {} & C_{exe}(i,j,k) \times E_x^{n}(i,j,k) + C_{exhz}(i,j,k) \\
& \times \left(H_z^{n+\frac{1}{2}}(i,j,k) - H_z^{n+\frac{1}{2}}(i,j-1,k) \right) \\
& + C_{exhy}(i,j,k) \left(H_y^{n+\frac{1}{2}}(i,j,k) \right. \\
& \left. - H_y^{n+\frac{1}{2}}(i,j,k-1) \right) + C_{exj}(i,j,k) \\
& \times J_{ix}^{n+\frac{1}{2}}(i,j,k)
\end{aligned}
\tag{1}
$$

FDTD equation for Electric Field in y-axis:

$$
\begin{aligned}
E_y^{n+1}(i,j,k) = {} & C_{eye}(i,j,k) \times E_y^{n}(i,j,k) + C_{eyhx}(i,j,k) \\
& \times \left(H_x^{n+\frac{1}{2}}(i,j,k) - H_x^{n+\frac{1}{2}}(i,j,k-1) \right) \\
& + C_{eyhz}(i,j,k) \\
& \times \left(H_z^{n+\frac{1}{2}}(i,j,k) - H_z^{n+\frac{1}{2}}(i-1,j,k) \right) \\
& + C_{eyj}(i,j,k) \times J_{iy}^{n+\frac{1}{2}}(i,j,k)
\end{aligned}
\tag{2}
$$

FDTD equation for Electric Field in z-axis:

$$
\begin{aligned}
E_z^{n+1}(i,j,k) = {} & C_{eze}(i,j,k) \times E_z^{n}(i,j,k) + C_{ezhy}(i,j,k) \\
& \times \left(H_y^{n+\frac{1}{2}}(i,j,k) - H_y^{n+\frac{1}{2}}(i,j,k-1) \right) \\
& + C_{ezhx}(i,j,k) \\
& \times \left(H_x^{n+\frac{1}{2}}(i,j,k) - H_x^{n+\frac{1}{2}}(i-1,j,k) \right) \\
& + C_{ezj}(i,j,k) \times J_{iz}^{n+\frac{1}{2}}(i,j,k)
\end{aligned}
\tag{3}
$$

FDTD equation for Magnetic Field in x-axis:

$$
\begin{aligned}
H_x^{n+\frac{1}{2}}(i,j,k) = {} & C_{hxh}(i,j,k) \times H_x^{n-\frac{1}{2}}(i,j,k) \\
& + C_{hxey}(i,j,k) \left(E_y^{n}(i,j,k+1) \right. \\
& \left. - E_y^{n}(i,j,k) \right) \\
& + C_{hxez}(i,j,k)\left(E_z^{n}(i,j+1,k) \right. \\
& \left. - E_z^{n}(i,j,k) \right) \times C_{hxm}(i,j,k) \times M_{ix}^{n}(i,j,k)
\end{aligned}
\tag{4}
$$

FDTD equation for Magnetic Field in y-axis

$$
\begin{aligned}
H_y^{n+\frac{1}{2}}(i,j,k) = {} & C_{hyh}(i,j,k) \times H_y^{n-\frac{1}{2}}(i,j,k) + C_{hyez}(i,j,k) \\
& \times \left(E_z^{n}(i+1,j,k) - E_z^{n}(i,j,k) \right) \\
& + C_{hyex}(i,j,k) \\
& \times \left(E_x^{n}(i,j,k+1) - E_x^{n}(i,j,k) \right) \\
& \times C_{hym}(i,j,k) \times M_{iy}^{n}(i,j,k)
\end{aligned}
\tag{5}
$$

FDTD equation for Magnetic Field in z-axis:

$$
\begin{aligned}
H_z^{n+\frac{1}{2}}(i,j,k) = {} & C_{hzh}(i,j,k) \times H_z^{n-\frac{1}{2}}(i,j,k) + C_{hzex}(i,j,k) \\
& \times \left(E_x^{n}(i,j+1,k) - E_x^{n}(i,j,k) \right) \\
& + C_{hzey}(i,j,k) \\
& \times \left(E_y^{n}(i+1,j,k) - E_y^{n}(i,j,k) \right) \\
& \times C_{hzm}(i,j,k) \times M_{iz}^{n}(i,j,k)
\end{aligned}
\tag{6}
$$

where *i*, *j*, *k* characterizes the index in Yee cell position along axis-x, axis-y, and axis-z

These six equations can be communicated utilizing a limited contrast estimation and revamp into six parts of the electric and attractive field with the regarding coefficient. Shortening the discretization of E_x electric field equation. For E_y and E_z electric field equations, the same practice is used. This is also related for H_x, H_y and H_z magnetic field equations, that apply the same style of practice.

Figure 2 demonstrates the flow chart of this work of the executed the technique of FDTD to construct the simulation tools. This procedure commenced with the literature reviewing on FDTD technique.

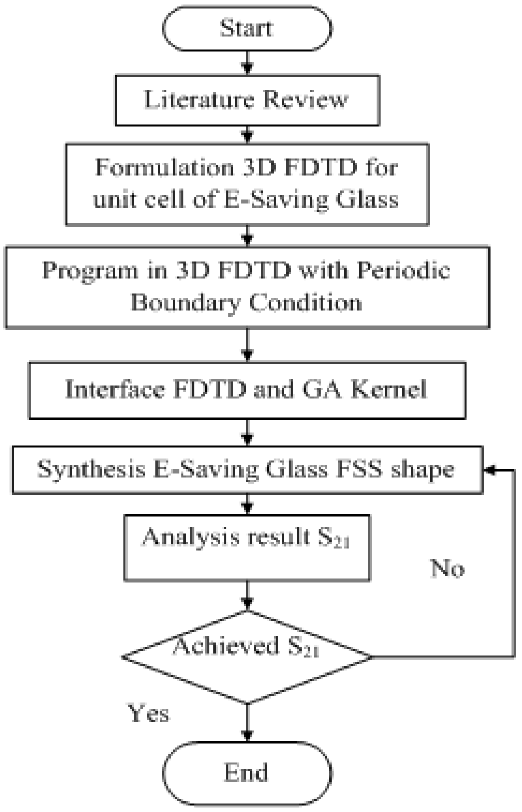

Figure 2. flow chart of implemented the technique of FDTD to develop simulation tools.

The applying to generate a population of solutions and some genetic operators had been applied, including mutation and crossover, to evolve the answers so that you can discover the quality one. The optimization tool enters included the wide variety of Yee cells, the kind of symmetry, the quantity of chromosome, the sort of complex, the kind of steel chromosome, and the form of cellular used in the structure in this study, as exposed within the Matlab code in Figure 3.

```
Cell=42% input unit cell length

sym=8 %type of symmetrical 4-quart, 8-octal, 0-no symmetry

numchro=1 % the numbers of chromosome

random=1 % 1-random, 0=no random

allone=0 % for unique chromosome, 1-for all chromosome is metal, 0-no chromosome is metal

HalfCell=Cell/2;
```

Figure 3: Matlab Code for GA optimization

III. FSS DESIGN

As for the regular form design, the metal oxide is covered on only some components of the glass. The proportion of coating is 30%, with glass without coating is 70%. From the share 30:70, it shows the possibility to signal replicate is better than the transmission signal. The metal oxide this is implemented on ESG on one aspect of the ordinary waft glass blocks the infrared rays but agrees on the white alerts [31]. Moreover, as a description of the ESG, the metal oxide covering layer does now not affect the prominence via the glass. The covering layer of ESG displays the warmth lower back into the structure that decreases heat loss via the opening hole.

In this system, typical form turned into designed for permit WLAN software. Figure 4 shows the steel patch for the FSS is perform in a rectangular loop shape. This design has been finalized in two alternative software of the CST and FORTRAN. The patch length, *L* is 12.0 mm with width, *W* of is 3.0 mm. there aren't any metal in the loop which. In this design, the loop is designed without metal.

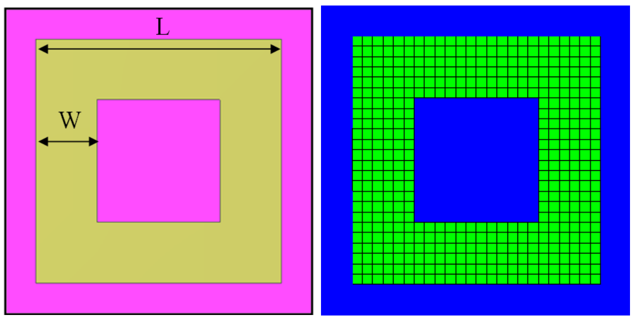

(a) (b)

Figure 4. FSS design of square loop shape, (a) in CST and (b) in FORTRAN software

Besides that, the second shaped that been apply in this work is a cross dipole, stated in Figure 5. Both designs had been applying in two different software of CST and FORTRAN, same as square loop-shaped. In this design, the incident electromagnetic wave is located points towards the middle part of the design with the dimension of 12 mm x 3 mm of length, *L* and width, *W*.

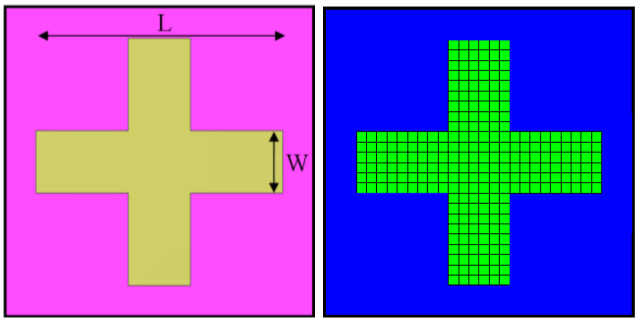

(b)

Figure 5. FSS design of cross dipole shape, (a) in CST and (b) in FORTRAN software

IV. RESULT

After the simulation work is done, the performance of this square loop-shaped is proven in Figure 6. From the determined, the graph outline has change differently among the FORTRAN and CST result. The result in FORTRAN shown the transmission coefficient of - 80 dB at 13.6 GHz of resonant frequency. The performance of the CST is achieved - 46.2 dB at 13.5 GHz with only 0.1 GHz slightly different of resonant frequency location compare with FORTRAN result. As the comparison, Esselle [22] was observed that - 22 dB transmission loss for both signals. Both simulators show the significant larger bandwidth with CST and FORTRAN shows the performance of 5.8 GHz and 5.1 GHz, respectively.

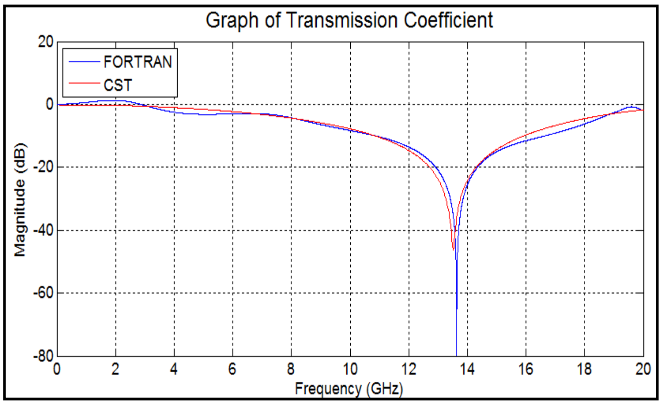

Figure 6. Graph of transmission coefficient for square loop FSS

The graph of transmission coefficient for cross dipole FSS is represented in Figure 7. In this graph, both illustrate the nearly same each other, with a little slight variance result at some points. The resonant frequency for both FDTD in FORTRAN and CST are 12.8 GHz with different transmission coefficient result of 68.1 dB and - 43.2 dB, respectively. For bandwidth, it shows 1.7 GHz for FORTRAN while 1.9 GHz in CST. On the other hand, 0 dB attenuation is exposed to cross dipole transmits WLAN. Compared with same style design of Kiani [19] in CST, the addition of ESG can improve the transmission at three different resonant frequency at 1.3 GHz, 2.45 GHz, and 5.0 GHz with - 9.0 dB, - 5.25 dB, and – 4.0 dB.

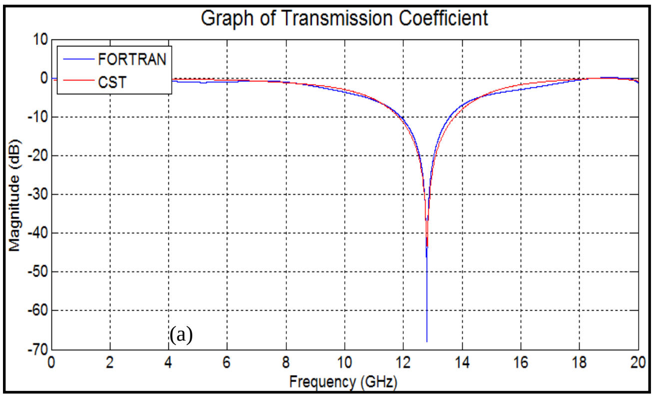

Figure 7. Graph of transmission coefficient for cross dipole FSS

V. CONCLUSION

In this work, the gap of research defines that two-different existing basic shape is used – the square loop shape FSS and another one is cross dipole shape FSS. After finished the simulation work for both FDTD in FORTRAN and CST simulator, it shows that the nearly same performance results on the transmission coefficient. In can be concluded that FDTD had been a suitable simulator to carry out a computational electromagnetic system for simulating the FSS design in Periodic Boundary Condition (PBC). For the future work, the other researcher can use the other complex or complicated design to ensure the acceptable result of the FSS design. The other researcher also can use another RF simulator such as HFSS simulator to compared with the previous CST and FORTRAN results performance.

ACKNOWLEDGMENT

The authors would like to thank Universiti Teknikal Malaysia Melaka (UTeM) for supporting in obtained the information and material in the development of our work. We also want to thank the Government of Malaysia which sponsoring this work under the TRGS/1/2014/ FKEKK/02/1/D00001 from Ministry of Higher Education (MOHE). Thanks also to UTeM Research and Innovation Management (CRIM) for the support of publication issues. Lastly, we also thank the anonymous referees whose comments led to an improved presentation of our work.

REFERENCES

[1] G. I. Kiani, K. L. Ford, L. G. Olsson, K. P. Esselle and C. J. Panagamuwa, "Switchable Frequency Selective Surface for Reconfigurable Electromagnetic Architecture of Buildings," in IEEE Transactions on Antennas and Propagation, vol. 58, no. 2, pp. 581-584, 2010.

[2] G. I. Kiani, A. Karlsson, L. Olsson and K. P. Esselle, "Glass Characterization for Designing Frequency Selective Surfaces to Improve Transmission through Energy Saving Glass Windows," 2007 Asia-Pacific Microwave Conference, pp. 1-4, 2007

[3] Pilkington, Pilkington Glass Handbook 2010, Pilkington Polska, 2010

[4] S. R. Hamid, B. C. Chew, M. A. Abdullah and Sarah-Halim, "Feasibility study of energy saving glass for Malaysian market," 3rd IET International Conference on Clean Energy and Technology 2014 (CEAT), pp. 1-4, 2014

[5] S. Habib, M. F. U. Butt and G. I. Kiani, "Parametric analysis of a band-pass FSS for double glazed soft-coated energy saving glass," 2015 International Symposium on Antennas and Propagation (ISAP), pp. 1-4. 2015

[6] F. Ma and L. Li, "Design of a Tri-bandpass FSS on dual-layer energy saving glass for improving RF transmission in green buildings," 2015

IEEE International Conference on Communication Problem-Solving (ICCP), pp. 405-407, 2015
[7] S. I. Sohail, K. P. Esselle and G. Kiani, "Design of a bandpass FSS on dual layer energy saving glass for improved RF communication in modern buildings," Proceedings of the 2012 IEEE International Symposium on Antennas and Propagation, pp. 1-2, 2012
[8] P. Ragulis, P. Ängskog, R. Simniškis, B. Vallhagen, M. Bäckström and Ž. Kancleris, "Shielding Effectiveness of Modern Energy-Saving Glasses and Windows," in IEEE Transactions on Antennas and Propagation, vol. 65, no. 8, pp. 4250-4258, 2017.
[9] H. S. Lim, "Fabrication of frequency selective structure and evaluation of microwave transmission on energy saving glass," master's thesis, Universiti Tun Hussein Onn Malaysia, 2015
[10] N. S. Mohamad, "A Study of Energy Efficiency Opportunities in Putrajaya Maritime Centre Towards Green Building," master's thesis, Universiti Tun Hussein Onn Malaysia, 2013
[11] M. Gustafsson, A. Karlsson, A. P. P. Rebelo and B. Widenberg, "Design of frequency selective windows for improved indoor-outdoor communication," in IEEE Transactions on Antennas and Propagation, vol. 54, no. 6, pp. 1897-1900, 2006.
[12] Singh, D., Kumar, A., Meena S. and Agarwala, V. Analysis of Frequency Selective Surface for Radar Absorbing Materials. Progress in Electromagnetics Research B, vol. 38, 297-314, 2012.
[13] E. A. Parker, A. D. Chuprin, J. C. Batchelor and S. B. Savia, "GA optimisation of crossed dipole FSS array geometry," in Electronics Letters, vol. 37, no. 16, pp. 996-997, 2001.
[14] Y. Zhao, Z. Zhang and Z. Feng, "A metallic Febry-Perot cavity antenna with slot-type FSS and hybrid lateral boundaries for high aperture efficiency," 2011 IEEE Electrical Design of Advanced Packaging and Systems Symposium (EDAPS), pp. 1-4, 2011
[15] G. I. Kiani, A. R. Weily and K. P. Esselle, "Frequency Selective Surface Absorber using Resistive Cross-Dipoles," 2006 IEEE Antennas and Propagation Society International Symposium, pp. 4199-4202, 2006
[16] F. Khosravi and P. Mousavi, "Bidirectional RHCP monopole slot antenna using Jerusalem-FSS polarization converter," 2013 IEEE Antennas and Propagation Society International Symposium (APSURSI), pp. 470-471, 2013
[17] H. Zahra, S. M. Abbas, M. F. Shafique and K. P. Esselle, "A switchable FSS based on modified Jerusalem-cross unit cell with extended top loading," 2015 International Symposium on Antennas and Propagation (ISAP), pp. 1-2, 2015
[18] T. Manabe, K. I. Kikuchi, S. Ochiai and T. Nishibori, "Dual-polarization Jerusalem-cross slot type FSS for a submillimeter-wave band," 2015 International Symposium on Antennas and Propagation (ISAP), pp. 1-3, 2015
[19] P. Majumdar, Z. Zhao, C. Ji and R. Liu, "Equivalent circuit model of multilayer double square loop FSS using vector-fitting," 2015 IEEE International Symposium on Antennas and Propagation & USNC/URSI National Radio Science Meeting, pp. 1276-1277, 2015
[20] F. C. Seman and N. K. Khalid, "Double square loop FSS with slots for closer band spacing at oblique incidence," 2014 IEEE Asia-Pacific Conference on Applied Electromagnetics (APACE), pp. 195-198, 2014
[21] G. Kiani, L. Olsson, A. Karlsson and K. Esselle, "Transmission analysis of energy saving glass windows for the purpose of providing FSS solutions at microwave frequencies," 2008 IEEE Antennas and Propagation Society International Symposium, pp. 1-4, 2008
[22] Y Ranga, L Matekovits, KP Esselle, AR Weily, The Use of a multi-layer frequency-selective-surface reflector to achieve antenna gain flatness over an ultra-wide band, 12th Australian Symposium on Antennas, 2011
[23] G. I. Kiani, L. G. Olsson, A. Karlsson, K. P. Esselle, and M. Nilsson, Cross-dipole bandpass frequency selective surface for energy-saving glass used in buildings, IEEE Transactions on Antennas and Propagation, Vol. 59, No. 2, 520-525, 2011.
[24] S. N. Azemi, K. Ghorbani, and W. S. T. Rowe, "3D Frequency Selective Surfaces," Progress in Electromagnetics Research C, vol. 29, pp. 191–203, 2012.
[25] D. Sharma and T. Shanmuganantham, "Design of miniaturised FSS microstrip antenna for Ku band applications," 2017 IEEE International Conference on Circuits and Systems (ICCS), pp. 316-318, 2017.
[26] H. Bodur, S. Ünaldı, S. Çimen and G. Çakır, "A novel reflectarray antenna combined with double layer FSS for RCS reduction," 2017 25th Telecommunication Forum (TELFOR), pp. 1-3, 2017.
[27] Y. S. Lee, F. Malek and F. H. Wee, "Investigate FSS structure effect on WIFI signal," 5th IET International Conference on Wireless, Mobile and Multimedia Networks (ICWMMN 2013), pp. 331-334, 2013
[28] B. Zhang, Xue Zheng-hui, Ren Wu and Sheng Xin-qing, "Analysis of periodic structures using FDTD method," Proceedings of the 9th International Symposium on Antennas, Propagation and EM Theory, pp. 864-867, 2010
[29] J. Chen, G. Hao and Q. H. Liu, "Using the ADI-FDTD Method to Simulate Graphene-Based FSS at Terahertz Frequency," in IEEE Transactions on Electromagnetic Compatibility, vol. 59, no. 4, pp. 1218-1223, 2017.
[30] J. Shunxi and D. Wenbin, "FDTD Analysis of Millimeter Wave FSS," 2006 Joint 31st International Conference on Infrared Millimeter Waves and 14th International Conference on Teraherz Electronics, Shanghai, pp. 306-306, 2006
[31] M. Bilal, R. Saleem, H. H. Abbasi, M. F. Shafique and A. K. Brown, "An FSS-Based Nonplanar Quad-Element UWB-MIMO Antenna System," in IEEE Antennas and Wireless Propagation Letters, vol. 16, pp. 987-990, 2017.